

1 **Title: Genetic variability in response to A β** 2 **deposition influences Alzheimer's risk**

3 4 **Authors:**

5 Dervis A. Salih¹, Sevinc Bayram¹, Manuel S. Guelfi², Regina Reynolds², Maryam
6 Shoi², Mina Ryten², Jonathan Brenton¹, David Zhang², Mar Matarin², Juan
7 Botia^{2,3}, Runil Shah², Keeley Brookes⁴, Tamar Guetta-Baranes⁴, Kevin Morgan⁴,
8 Eftychia Bellou⁵, Damian M. Cummings¹, John Hardy^{2*}, Frances A. Edwards¹,
9 Valentina Escott-Price⁵.

10 11 **Affiliations:**

12 ¹Department of Neuroscience, Physiology and Pharmacology, UCL, Gower Street,
13 London WC1E 6BT, UK.

14
15 ²Reta Lila Research Laboratories and Department of Molecular Neuroscience,
16 Institute of Neurology, UCL, 1 Wakefield Street, London WC1N 1PJ, UK.

17
18 ³Department of Information and Communications Engineering, Universidad de
19 Murcia, Spain.

20
21 ⁴Human Genetics, School of Life Sciences, Life Sciences Building, University Park,
22 University of Nottingham, Nottingham NG7 2RD, UK.

23
24 ⁵Institute of Psychological Medicine and Clinical Neurosciences, MRC Centre for
25 Neuropsychiatric Genetics and Genomics, Cardiff University, UK.

26
27 * Correspondence to: j.hardy@ucl.ac.uk
28
29
30

Abstract:

Genetic analysis of late-onset Alzheimer's disease risk has previously identified a network of largely microglial genes that form a transcriptional network. In transgenic mouse models of amyloid deposition we have previously shown that the expression of many of the mouse orthologs of these genes are co-ordinately up-regulated by amyloid deposition. Here we investigate whether systematic analysis of other members of this mouse amyloid-responsive network predicts other Alzheimer's risk loci. This statistical comparison of the mouse amyloid-response network with Alzheimer's disease genome-wide association studies identifies 5 other genetic risk loci for the disease (*OAS1*, *CXCL10*, *LAPTM5*, *ITGAM* and *LILRB4*). This work suggests that genetic variability in the microglial response to amyloid deposition is a major determinant for Alzheimer's risk.

One Sentence Summary:

Identification of 5 new risk loci for Alzheimer's by statistical comparison of mouse A β microglial response with gene-based SNPs from human GWAS

58 Main Text:

59 All the mutations in the genes causing early-onset Alzheimer's disease (AD) alter
60 APP processing such that amyloid deposition becomes more likely (1). In
61 contrast, with the exception of some rare variants in APP processing enzymes (2-
62 5), the majority of the risk in late-onset disease has been shown to be due to
63 sequence variability in genes expressed in the innate immune system (largely
64 microglial) and lipid metabolism (6). When we identified the microglial gene
65 *TREM2* (7) as a potent risk gene for late-onset disease, we confirmed earlier
66 reports that its expression was strongly increased by amyloid deposition in *APP*
67 transgenic mice (7-10). In a genome-wide expression study of transgenic
68 *APP/PSEN1* mice during pathology development, we noted that *Trem2* was one
69 of the genes whose expression was up-regulated the most in relation to amyloid
70 deposition and that *Trem2* expression showed a strong correlation with an
71 entire network of genes co-expressed in the innate immune system. This
72 immune module of genes showed a remarkable correlation to amyloid pathology
73 and contained orthologs of other established Alzheimer's risk genes such as
74 *Abca7* and *Ms4a6d* (correlation = 0.87; $p = 6e^{-32}$)(9, 11). Notably, the two AD risk
75 loci for *ABI3* and *PLCG2* identified subsequent to our study were also present in
76 this network (12), suggesting that this amyloid-responsive immune network may
77 predict future risk genes for AD.

78 An important outstanding question is whether late-onset AD is mostly due to an
79 inadequate cellular response to rising A β and its deposition, particularly due to
80 sequence and expression variability in genes expressed by the innate immune
81 system and/or involved in lipid processing. This hypothesis is difficult to study
82 in human post-mortem tissue because after an extended period of disease the
83 proportion of cell types in the brain have changed and the remaining cells show
84 extensive compensatory changes in gene expression. With these questions in
85 mind, we determined whether surveying the gene expression network that
86 responds robustly to amyloid pathology could be used to identify further AD risk
87 loci. Although amyloid mouse models have clear limitations in that they do not
88 show tau tangles or neuronal loss, they allow us to study the time-course
89 response of a healthy innate immune system reacting to A β , in which the innate

immune cells have the ability to ultimately prevent A β killing neurons. Our previous expression network was constructed using expression arrays (9). Because these microarrays are limited by their probe content and have a limited dynamic range, we have now sequenced the transcriptome using RNA-seq and reconstructed a higher resolution expression network. The new full microglial module of genes shows a dramatic correlation with A β pathology (correlation = 0.94; $p < 3e^{-41}$), and contains the mouse orthologs of existing GWAS loci *TREM2*, *ABI3*, *CD33*, *INPP5D*, *MS4A6D*, *SPI1*, *PLCG2*, *RIN3*, *HLA* and *APOE* (Table S1). The genes showing the tightest expression correlation/A β -response within the module form the network shown in Fig. 1 and Table S2 (top 147 genes from a total of 1,584 genes with up-regulated expression as part of the immune module based on the topological overlap measure, TOM, see Methods). This network is broadly similar to the network derived from the analysis of the same RNA by microarray methods (9), and importantly closely resembles microglial networks published by other groups using different amyloid mouse models (13-17), suggesting this is a conserved network of genes that can be reliably identified using different methodologies. *Trem2* forms a hub gene in our network indicating that *Trem2* expression is highly correlated to many other genes in the network, and may drive the expression response of this network. In line with this idea, *Trem2* has been shown to regulate at least part of this immune module (13, 14, 16). The network we identified also is broadly similar to a human network of immune genes containing *TYROBP*, *TREM2*, *MS4A* family genes, *C1Q* members and *CD33*, identified from human pathology tissue bearing in mind the caveats discussed above (18, 19), suggesting this mouse A β -response gene network behaves similarly in humans.

Within our mouse immune network, we first confirmed that several members were orthologs of AD loci variants using the data from the Alzheimer's disease genetic consortium (11, 20)(Table 1). We then asked whether the other members of the mouse microglial amyloid-response network overlapped with individual human genes containing multiple SNPs associated with AD by cross-referencing gene-based statistical approaches (20). Overall, we found there was an enrichment of human genes with significant AD-associated SNPs within this amyloid-responsive network. This enrichment was more than would be

expected by chance alone, even after the established GWAS loci were excluded ($p = 1.91 \times 10^{-5}$ for highly connected network genes, Fig. 1, top 147 genes, versus $p = 7.32 \times 10^{-4}$ for the entire module of 1,584 genes, Table S1). As a comparison to the mouse amyloid-responsive network, the mouse tau-responsive immune network was not significantly enriched for human genes with AD-associated SNPs when the central portion of the tau network containing the highly connected genes were considered, after the established GWAS loci were excluded as before ($p = 0.92$), although *ApoE* is part of this module (Fig. S1, top 137 genes from a total of 2,299 genes in the immune module based on the TOM). When the entire module of tau-responsive immune genes (2,299 genes) was considered there was a significant enrichment, $p = 4.63 \times 10^{-6}$, suggesting that a proportion of AD-associated SNPs appear in microglial genes that have mouse orthologs, but are less responsive to tau pathology compared to amyloid pathology. The amyloid network analyses identified 5 genes within the mouse microglial network whose human orthologs contained SNPs significantly associated with AD, counting the genes within 0.5 Mb as one locus (see Methods, 20). These 5 genes, *OAS1*, *CXCL10*, *LAPTM5*, *ITGAM* and *LILRB4*, have not been previously reported as having variants significantly associated with AD using traditional GWAS approaches (Table 1, Fig. S2-4). Indeed the amyloid-responsive sub-network of these 5 novel genes with the established GWAS loci *TREM2*, *ABI3*, *CD33*, *INPP5D*, *SPI1* and *MS4A6D* (Fig. 1) is not highly connected in an innate immune gene network associated with tau pathology (Fig. S1), suggesting this sub-network is more responsive to amyloid pathology than other pathologies. Furthermore, in common with the existing 6 known GWAS-associated genes, the 5 novel genes we identify respond very early to A β deposition, with gene expression increasing from 4 months of age in the homozygous *APP/PSEN1* mice (Fig. S5).

Aspects of the amyloid-responsive network we identify in our analysis containing the 5 new genes with the existing 6 GWAS loci are broadly similar to microglial networks we and others have previously identified in human brain analyses. Zhang and colleagues identified an AD-relevant network centered on *TYROBP* and *TREM2* which contained *ITGAM* and *LAPTM5* (18) and we described a human microglial network containing *LAPTM5*, *ITGAM* and *LILRB4* (19). We then determined whether these novel Alzheimer's risk loci, derived from a

mouse A β -response network were present in independent datasets of human brain co-expression networks. Cross referencing the network (see Methods) with the data from the ROS/MAP project (21, 22), and BRAINEAC (23) datasets revealed that *LAPTM5*, *ITGAM* and *LILRB4* clustered together in the same network in the ROSMAP based co-expression networks, together with many of the GWAS risk genes for AD, and with *SPI1*, the myeloid cell transcription factor (24)(Fig. S6; Fisher's Exact test Bonferroni corrected $p = 1.34 \times 10^{-13}$ for AD). We confirmed these module memberships in the BRAINEAC data for control brains generated in our own lab and found essentially the same results (data not shown). Interestingly, we found that SPI1 was bound to the regulatory regions of *Laptm5* and *Itgam*, along with binding to established AD risk gene orthologs *Trem2*, *Abi3*, *Inpp5d*, *Ms4a6d* and *Spi1* itself, by searching data from a chromatin immunoprecipitation experiment against SPI1 in mouse microglial-like BV-2 cells (25). This finding was supported by mining for regulatory features and *cis*-regulatory modules in the amyloid-response network genes using *i-cisTarget* that uses a vast library of regulatory data (26). Together, these findings suggest that a number of the predicted and established AD risk genes may be regulated by SPI1, which itself alters AD risk by coordinating a program of microglial-expressed genes (24).

Since most GWAS loci are thought to operate by regulating the expression of neighboring genes (24, 27, 28), for each of the 5 potential AD-associated genes we performed a colocalisation analysis to test the association between AD loci located within these genes and loci regulating these genes' expression (eQTLs; (29). eQTLs were obtained from two previously published datasets using baseline and stimulated human-derived monocytes and iPSC-derived macrophages (30, 31). In these studies, macrophages and monocytes were stimulated with various immunostimulants to activate distinct, well-characterised immune signaling pathways, including those broadly associated with bacterial and viral responses. Interestingly, we identified 3 colocalisations between AD loci and eQTLs regulating *OAS1* gene expression, all of which were identified in stimulated states, suggesting that this association is only active in certain environmental conditions (Fig. 2 and Fig. S7-8), in particular those

designed to model monocyte/macrophage priming or more chronic inflammation.

Surveying the literature on our genes of interest revealed that *OAS1* (2-prime,5-prime oligoadenylate synthetase 1) is involved in the regulation of cytokine expression (32). *OAS1* is induced by interferons (33), which supports our eQTL analysis showing that the best SNP we identified for *OAS1* appears in a locus which acts as an eQTL in response to interferon- γ (IFN γ ; Fig. 2 and Fig. S7-8). *OAS1* can additionally activate Ribonuclease L which degrades viral RNA and inhibits viral replication (33). *CXCL10* (IP-10; chemokine, CXC motif, ligand 10) is a proinflammatory cytokine that has been reported to have increased concentrations in the AD-brain, particularly associated with amyloid plaques (34), and *CXCL10* increases plaque pathology in *APP/PSEN1* transgenic mice (35). *CXCL10* was found to increase in older people and in AD, and correlated with cognitive decline (36). *LAPTM5* (lysosome-associated protein, transmembrane 5) is associated with amyloid pathology in transgenic mice (17), and *LILRB4* (leukocyte immunoglobulin-like receptor, subfamily B, member 4), has also been shown to be increased with amyloid pathology and specifically associated with amyloid plaques (15, 37, 38). The functions of *LAPTM5* and *LILRB4* have not been well characterized, but are thought to suppress the activation of a variety of immune cells. *ITGAM* (alpha-chain subunit of the heterodimeric integrin complement receptor alpha-M-beta-2, also known as CD11b or CR3A), is a cell surface receptor involved in activation, migration and phagocytosis of immune cells, so much so that *ITGAM* is used as a marker of activated microglia (37, 39, 40), and is involved in systemic lupus (41). *ITGAM* was highlighted in recent genetic and functional analyses as being a likely AD risk gene, whose expression was driven by *SPI1*, and related to amyloid pathology in mice and humans (17, 18, 24, 37, 42, 43).

The importance of this work is two fold. First, by identifying more genetic loci involved in pathogenesis, we derive a more complete insight into the cellular processes and molecular mechanisms underlying the disease. In this regard this work is complementary to that of Huang and colleagues (24), showing that microglial *SPI1*-driven transcription is a common feature of many Alzheimer's

loci. These findings are also consistent with previous work on *Trem2* (8, 13, 14, 16, 44) and *CD33* (27, 28) suggesting these risk genes are crucial in controlling the microglial response to amyloid-induced damage. Understanding the mechanisms of function of TREM2 and the amyloid-responsive sub-network identified here may be useful for leveraging therapeutic opportunities. Second, and perhaps of greater importance, this work implies that, overall, how well an individual responds to amyloid deposition at the cellular and gene expression level plays a large part in determining ones risk of disease, and this may be used to predict the chances of developing AD before irreversible neurodegeneration sets in.

URLs of databases used:

Mouseac: www.mouseac.org
 Braineac: www.braineac.org
 1,000 genomes: <http://www.1000genomes.org/> and
<http://www.internationalgenome.org/>
 Coloc: <https://github.com/chr1swallace/coloc>
 Bioconductor: <https://bioconductor.org/biocLite.R>
 ROS/MAP: <https://www.synapse.org/#!Synapse:syn3219045>
 i-CisTarget: <https://gbiomed.kuleuven.be/apps/lcb/i-cisTarget/>
 GTEx V6 gene expression: <https://gtexportal.org/home/>
 Coexp: <https://github.com/juanbot/coexp>

Methods:

Mouse and transcriptome work

Total RNA was used from the same mice as described in Matarin *et al.* (9). The quality and concentration of the total RNA was assessed using capillary electrophoresis of each sample. RNA-seq library preparation and sequencing was performed by Eurofins Genomics (strand-specific cDNA libraries with polyA selection), by Illumina (HiSeq 2500) sequencing (2x 100 bp paired-end; multiplex 12 samples per lane - 28M reads). Adaptors and low quality base pairs were removed from FASTQ files using Trim Galore (Babraham Bioinformatics).

Transcripts were quantified with Salmon (45), using gene annotation from ENSEMBL GRCm38. Salmon was used because it incorporates GC correction and accounts for fragment positional bias. To get gene level quantification from the transcripts, and correct for average transcript length and library size, expressed as transcripts per million (TPM), the tximport R package was used (46). TPM values were log2 transformed, and genes were considered expressed when log2 TPM values displayed a mean >1.5 for a given gene for at least one group of mice, when gene TPM values were averaged for each genotype at each age (resulting in a total of 18,562 genes expressed).

Weighted co-expression network analyses (WGCNAs) was performed as described in Matarin *et al.* (9). Coexpression networks were built using the WGCNA package in R. Genes with variable expression patterns (coefficient of variation >5% for wild-type and amyloid mice, or wild-type and tau mice) from normalized log2 TPM values were selected for network analyses resulting in 13,536 genes for network analyses (47-50). The module of genes with the highest significant correlation with amyloid or tau pathology was selected for analysis (amyloid, correlation 0.94, $p = 3e-41$; tau, correlation 0.82, $p = 4e-12$). TOM connectivity values were used to plot the network diagrams (TOM > 0.39 for amyloid-responsive module, and TOM > 0.36 for tau-responsive module). Hub genes were considered to be those with at least 15 connections to other genes.

Genetic Analysis

The lists of mouse genes were converted to the lists of human genes using convertMouseGeneList() function, library biomaRt in R downloaded from <https://bioconductor.org/biocLite.R>.

The significance of the association of human genes to AD was assessed as described in (20). Briefly, the IGAP (11) summary statistics calculated for each SNP in a sample of 17,008 AD cases and 37,154 controls were used to derive the gene-based p-values. SNPs were assigned to genes if they were located within the genomic sequence lying between the start of the first and the end of the last exon of any transcript corresponding to that gene. The chromosome and location

for all currently known human SNPs along with their assignment to genes were taken from the dbSNP132 database (build 37.1). If a SNP belongs to more than one gene, it was assigned to each of these genes. Data from the 1,000 genomes project (release Dec2010) were used as a reference panel for both (a) SNP imputation, and (b) calculation of LD between markers (51). An approximate statistical approach (52) which controls for LD and different number of markers per gene, was used to derive the gene-based p-values. Prior to the gene-based analyses all individual SNP p-values were corrected for genomic control.

We calculated the significance of the excess *number* of genes attaining the specified thresholds (0.05, 0.01 and 0.001) based upon the assumption that, under the null hypothesis of no association, the number of significant genes at a significance level of α in a scan is distributed as a binomial (N, α), where N is the total number of genes, assuming that genes are independent. Genes within 0.5Mb of each other are counted as one signal when calculating the observed number of *significant* genes. This prevents significance being inflated by LD between genes, where a single association signal gives rise to several significantly-associated genes. The over-representation p-value was calculated using a Z-test comparing the number of observed independent significant genes with the expected number of significant genes with corresponding variance ($=N*a*(1-a)$), where N is the total number of independent genes in the network, and a is the significance threshold). We report the genes at the gene-based p-value threshold 0.01, where the excess of observed significant genes was the highest.

Human sample co-expression network construction and annotation

We generated co-expression networks from RNA-seq based gene expression profiling of 635 pre-frontal cortex samples from the ROS/MAP project (21, 22, 53). We used cognitive decline as a covariate to construct four networks: all samples network, not AD, probable AD and AD. We used WGCNA (50) with an optimization for constructing more biologically meaningful co-expression networks (54). We corrected for batch effects using ComBAT (55), obtained unknown hidden effect covariates with SVA (56), and used the residuals obtained by regressing the gene expression with SVA covariates, age and gender.

Then we annotated the network modules for enrichment of Gene Ontology, REACTOME (57), and KEGG (58) pathways using gProfileR (59).

Colocalisation with monocyte eQTL data sets

We applied coloc (version 3.1, see URLs) to test for colocalisation between AD loci surrounding the five novel identified genes (*OAS1*, *CXCL10*, *LAPTM5*, *ITGAM*, and *LILRB4*) and eQTLs (29). While no microglial eQTL datasets exist to date, eQTL analyses have been performed using monocytes and iPSC-derived macrophages (at rest and stimulated with various immunostimulants, such as IFN- γ)(30, 31). We ran coloc using default parameters and priors on all SNPs that: 1) had eQTLs tagging one of the 5 novel genes (this included all tested SNP-gene associations, including non-significant eQTLs); and 2) had overlapping SNPs in the AD GWAS. We excluded all loci in which $PP3 + PP4 < 0.8$, to exclude loci where we were underpowered to detect colocalisation. Loci with $PP4/PP3 \geq 2$ were considered colocalised due to a single shared causal variant (PP4), as opposed to two distinct causal variants (PP3).

Fig. 1. Amyloid-responsive immune network of genes featuring several orthologs of established GWAS variants associated with AD, predicts the importance of five new genes that may influence the risk of developing AD.

Network plot using VisANT reveals key drivers of an immune module from RNA-seq derived gene expression from the hippocampus of wild-type and amyloid mice. Red circles show established GWAS genes associated with AD including *Trem2*, *Cd33*, *Abi3* and *Spi1*. Blue underline shows genes predicted to confer increased risk of AD by overlapping strongly amyloid-responsive gene expression data in amyloid mice with analyses identifying combinations of adjacent human SNPs within individual genes showing significant associations with AD (see Methods, 20). Genes shown in this network display up-regulated expression in response to amyloid deposition. Larger red spheres represent “hub genes,” those showing the greatest number of connections to other genes in the network, and include *Trem2*, *Tryobp*, *Lilrb4a*, *P2ry13*, *Ctss*, *Ctsz*, *Mpeg1* and *Plek*, which are likely to play important roles in driving microglial function.

Fig. 2. Colocalisation of AD GWAS loci with eQTLs derived from baseline and stimulated iPSC-derived macrophages. Colocalisation of AD loci and eQTLs targeting *OAS1* in baseline and stimulated states (IFN γ and Salmonella, 18 and 5 hours respectively). In the eQTL panels, grey and red data points represent macrophages at baseline or stimulated with both IFN γ and Salmonella, respectively. The best AD locus in *OAS1*, rs1131454 (p-value = 3.92×10^{-5}), is highlighted with the black line. IFN γ , interferon- γ . Numerical results are reported in Table S3.

Table 1. The genes predicted to contain SNP variants associated with AD together with established loci associated with AD from GWAS. Genes predicted to confer increased risk of AD by overlapping strongly amyloid-responsive gene expression data in amyloid mice (Fig. 1) with analyses identifying combinations of adjacent human SNPs within individual genes showing significant associations with AD (see Methods; 20). The SNP positions are provided for build 37, assembly Hg19, as in IGAP study (11). The SNP with

the most significant p-value within each gene is denoted as 'Best SNP,' from the IGAP stage 1 dataset. The effect size (coefficient of the logistic regression) is provided for the best reported SNP from IGAP data; a positive number indicates that the allele increases risk of AD, and so a negative number indicates the allele is protective. The allele frequency from the IGAP study is also provided. The established genes altering risk for AD from GWAS are given for comparison.

References:

1. J. Hardy, D. J. Selkoe, The amyloid hypothesis of Alzheimer's disease: progress and problems on the road to therapeutics. *Science* **297**, 353-356 (2002).
2. M. Kim *et al.*, Potential late-onset Alzheimer's disease-associated mutations in the ADAM10 gene attenuate {alpha}-secretase activity. *Hum Mol Genet* **18**, 3987-3996 (2009).
3. B. W. Kunkle *et al.*, Meta-analysis of genetic association with diagnosed Alzheimer's disease identifies novel risk loci and implicates Abeta, Tau, immunity and lipid processing. *bioRxiv*, (2018). doi 10.1101/294629
4. I. Jansen *et al.*, Genetic meta-analysis identifies 9 novel loci and functional pathways for Alzheimers disease risk. *bioRxiv*, (2018). doi 10.1101/258533
5. R. E. Marioni *et al.*, GWAS on family history of Alzheimer's disease. *Transl Psychiatry* **8**, 99 (2018).
6. L. Jones *et al.*, Genetic evidence implicates the immune system and cholesterol metabolism in the aetiology of Alzheimer's disease. *PLoS One* **5**, e13950 (2010).
7. R. Guerreiro *et al.*, TREM2 variants in Alzheimer's disease. *The New England journal of medicine* **368**, 117-127 (2013).
8. P. J. Cheng-Hathaway *et al.*, The Trem2 R47H variant confers loss-of-function-like phenotypes in Alzheimer's disease. *Molecular neurodegeneration* **13**, 29 (2018).
9. M. Matarin *et al.*, A genome-wide gene-expression analysis and database in transgenic mice during development of amyloid or tau pathology. *Cell Rep* **10**, 633-644 (2015).
10. W. M. Song *et al.*, Humanized TREM2 mice reveal microglia-intrinsic and -extrinsic effects of R47H polymorphism. *The Journal of experimental medicine* **215**, 745-760 (2018).
11. J. C. Lambert *et al.*, Meta-analysis of 74,046 individuals identifies 11 new susceptibility loci for Alzheimer's disease. *Nat Genet* **45**, 1452-1458 (2013).
12. R. Sims *et al.*, Rare coding variants in PLCG2, ABI3, and TREM2 implicate microglial-mediated innate immunity in Alzheimer's disease. *Nat Genet* **49**, 1373-1384 (2017).

- 415 13. H. Keren-Shaul *et al.*, A Unique Microglia Type Associated with Restricting
416 Development of Alzheimer's Disease. *Cell* **169**, 1276-1290 e1217 (2017).
- 417 14. C. Y. D. Lee *et al.*, Elevated TREM2 Gene Dosage Reprograms Microglia
418 Responsivity and Ameliorates Pathological Phenotypes in Alzheimer's
419 Disease Models. *Neuron* **97**, 1032-1048 e1035 (2018).
- 420 15. E. Castillo *et al.*, Comparative profiling of cortical gene expression in
421 Alzheimer's disease patients and mouse models demonstrates a link
422 between amyloidosis and neuroinflammation. *Scientific reports* **7**, 17762
423 (2017).
- 424 16. Y. Wang *et al.*, TREM2 Lipid Sensing Sustains the Microglial Response in
425 an Alzheimer's Disease Model. *Cell* **160**, 1061-1071 (2015).
- 426 17. K. N. Nam *et al.*, Integrated approach reveals diet, APOE genotype and sex
427 affect immune response in APP mice. *Biochim Biophys Acta* **1864**, 152-
428 161 (2018).
- 429 18. B. Zhang *et al.*, Integrated systems approach identifies genetic nodes and
430 networks in late-onset Alzheimer's disease. *Cell* **153**, 707-720 (2013).
- 431 19. P. Forabosco *et al.*, Insights into TREM2 biology by network analysis of
432 human brain gene expression data. *Neurobiology of Aging* **34**, 2699-2714
433 (2013).
- 434 20. V. Escott-Price *et al.*, Gene-wide analysis detects two new susceptibility
435 genes for Alzheimer's disease. *PLoS One* **9**, e94661 (2014).
- 436 21. P. L. De Jager *et al.*, A multi-omic atlas of the human frontal cortex for
437 aging and Alzheimer's disease research. *Sci Data* **5**, 180142 (2018).
- 438 22. D. A. Bennett, J. A. Schneider, Z. Arvanitakis, R. S. Wilson, Overview and
439 findings from the religious orders study. *Curr Alzheimer Res* **9**, 628-645
440 (2012).
- 441 23. A. Ramasamy *et al.*, Genetic variability in the regulation of gene
442 expression in ten regions of the human brain. *Nat Neurosci* **17**, 1418-1428
443 (2014).
- 444 24. K. L. Huang *et al.*, A common haplotype lowers PU.1 expression in myeloid
445 cells and delays onset of Alzheimer's disease. *Nat Neurosci* **20**, 1052-1061
446 (2017).
- 447 25. J. Satoh, N. Asahina, S. Kitano, Y. Kino, A Comprehensive Profile of ChIP-
448 Seq-Based PU.1/Spi1 Target Genes in Microglia. *Gene Regul Syst Bio* **8**,
449 127-139 (2014).
- 450 26. H. Imrichova, G. Hulselmans, Z. K. Atak, D. Potier, S. Aerts, i-cisTarget 2015
451 update: generalized cis-regulatory enrichment analysis in human, mouse
452 and fly. *Nucleic Acids Res* **43**, W57-64 (2015).
- 453 27. A. Griuciu *et al.*, Alzheimer's disease risk gene CD33 inhibits microglial
454 uptake of amyloid beta. *Neuron* **78**, 631-643 (2013).
- 455 28. E. M. Bradshaw *et al.*, CD33 Alzheimer's disease locus: altered monocyte
456 function and amyloid biology. *Nat Neurosci* **16**, 848-850 (2013).
- 457 29. C. Giambartolomei *et al.*, Bayesian test for colocalisation between pairs of
458 genetic association studies using summary statistics. *PLoS Genet* **10**,
459 e1004383 (2014).
- 460 30. S. Kim-Hellmuth *et al.*, Genetic regulatory effects modified by immune
461 activation contribute to autoimmune disease associations. *Nat Commun* **8**,
462 266 (2017).

- 463 31. K. Alasoo *et al.*, Shared genetic effects on chromatin and gene expression
464 indicate a role for enhancer priming in immune response. *Nat Genet* **50**,
465 424-431 (2018).
- 466 32. W. B. Lee *et al.*, OAS1 and OAS3 negatively regulate the expression of
467 chemokines and interferon-responsive genes in human macrophages.
468 *BMB Rep*, in press (2018).
- 469 33. J. Donovan, M. Dufner, A. Korennykh, Structural basis for cytosolic double-
470 stranded RNA surveillance by human oligoadenylate synthetase 1. *Proc*
471 *Natl Acad Sci U S A* **110**, 1652-1657 (2013).
- 472 34. R. S. Duan *et al.*, Decreased fractalkine and increased IP-10 expression in
473 aged brain of APP(swe) transgenic mice. *Neurochem Res* **33**, 1085-1089
474 (2008).
- 475 35. M. Krauthausen *et al.*, CXCR3 promotes plaque formation and behavioral
476 deficits in an Alzheimer's disease model. *The Journal of clinical*
477 *investigation* **125**, 365-378 (2015).
- 478 36. S. Bradburn *et al.*, Dysregulation of C-X-C motif ligand 10 during aging and
479 association with cognitive performance. *Neurobiol Aging* **63**, 54-64
480 (2018).
- 481 37. W. Kamphuis, L. Kooijman, S. Schetters, M. Orre, E. M. Hol, Transcriptional
482 profiling of CD11c-positive microglia accumulating around amyloid
483 plaques in a mouse model for Alzheimer's disease. *Biochim Biophys Acta*
484 **1862**, 1847-1860 (2016).
- 485 38. K. T. Wirz *et al.*, Cortical beta amyloid protein triggers an immune
486 response, but no synaptic changes in the APPswe/PS1dE9 Alzheimer's
487 disease mouse model. *Neurobiol Aging* **34**, 1328-1342 (2013).
- 488 39. Y. Matsuoka *et al.*, Inflammatory responses to amyloidosis in a transgenic
489 mouse model of Alzheimer's disease. *The American journal of pathology*
490 **158**, 1345-1354 (2001).
- 491 40. M. T. Heneka *et al.*, NLRP3 is activated in Alzheimer's disease and
492 contributes to pathology in APP/PS1 mice. *Nature* **493**, 674-678 (2013).
- 493 41. J. M. Anaya *et al.*, Evaluation of genetic association between an ITGAM
494 non-synonymous SNP (rs1143679) and multiple autoimmune diseases.
495 *Autoimmun Rev* **11**, 276-280 (2012).
- 496 42. A. Olmos-Alonso *et al.*, Pharmacological targeting of CSF1R inhibits
497 microglial proliferation and prevents the progression of Alzheimer's-like
498 pathology. *Brain* **139**, 891-907 (2016).
- 499 43. S. Hong *et al.*, Complement and microglia mediate early synapse loss in
500 Alzheimer mouse models. *Science* **352**, 712-716 (2016).
- 501 44. F. Mazaheri *et al.*, TREM2 deficiency impairs chemotaxis and microglial
502 responses to neuronal injury. *EMBO Rep* **18**, 1186-1198 (2017).
- 503 45. R. Patro, G. Duggal, M. I. Love, R. A. Irizarry, C. Kingsford, Salmon provides
504 fast and bias-aware quantification of transcript expression. *Nature*
505 *methods* **14**, 417-419 (2017).
- 506 46. C. Soneson, M. I. Love, M. D. Robinson, Differential analyses for RNA-seq:
507 transcript-level estimates improve gene-level inferences. *F1000Res* **4**,
508 1521 (2015).
- 509 47. S. Horvath *et al.*, Analysis of oncogenic signaling networks in glioblastoma
510 identifies ASPM as a molecular target. *Proc.Natl.Acad.Sci.U.S.A* **103**,
511 17402-17407 (2006).

48. M. C. Oldham, S. Horvath, D. H. Geschwind, Conservation and evolution of gene coexpression networks in human and chimpanzee brains. *Proc.Natl.Acad.Sci.U.S.A* **103**, 17973-17978 (2006).
49. B. Zhang, S. Horvath, A general framework for weighted gene co-expression network analysis. *Stat Appl Genet Mol Biol* **4**, Article17 (2005).
50. P. Langfelder, S. Horvath, WGCNA: an R package for weighted correlation network analysis. *BMC.Bioinformatics.* **9**, 559 (2008).
51. C. Genomes Project *et al.*, A global reference for human genetic variation. *Nature* **526**, 68-74 (2015).
52. V. Moskvina, M. C. O'Donovan, Detailed analysis of the relative power of direct and indirect association studies and the implications for their interpretation. *Hum Hered* **64**, 63-73 (2007).
53. D. A. Bennett *et al.*, Overview and findings from the rush Memory and Aging Project. *Curr Alzheimer Res* **9**, 646-663 (2012).
54. J. A. Botia *et al.*, An additional k-means clustering step improves the biological features of WGCNA gene co-expression networks. *BMC Syst Biol* **11**, 47 (2017).
55. W. E. Johnson, C. Li, A. Rabinovic, Adjusting batch effects in microarray expression data using empirical Bayes methods. *Biostatistics (Oxford, England)* **8**, 118-127 (2007).
56. J. T. Leek, J. D. Storey, Capturing heterogeneity in gene expression studies by surrogate variable analysis. *PLoS Genet* **3**, 1724-1735 (2007).
57. A. Fabregat *et al.*, The Reactome Pathway Knowledgebase. *Nucleic Acids Res* **46**, D649-D655 (2018).
58. M. Kanehisa, Y. Sato, M. Kawashima, M. Furumichi, M. Tanabe, KEGG as a reference resource for gene and protein annotation. *Nucleic Acids Res* **44**, D457-462 (2016).
59. J. Reimand, M. Kull, H. Peterson, J. Hansen, J. Vilo, g:Profiler--a web-based toolset for functional profiling of gene lists from large-scale experiments. *Nucleic Acids Res* **35**, W193-200 (2007).

Acknowledgements:

DAS and FAE are funded by ARUK. JH and VEP are members of the UKDRI. JH and FAE are supported by the Cure Alzheimer's Fund, JH is supported by the Dolby Foundation. The University of Nottingham Group is funded by ARUK and hosts the ARUK Consortium DNA Bank, with the following members: Tulsi Patel¹, David M. Mann², Peter Passmore³, David Craig³, Janet Johnston³, Bernadette McGuinness³, Stephen Todd³, Reinhard Heun³, Heike Kölsch⁵, Patrick G. Kehoe⁶, Emma R.L.C. Vardy⁷, Nigel M. Hooper², Stuart Pickering-Brown², Julie Snowden⁸, Anna Richardson⁸, Matt Jones⁸, David Neary⁸, Jenny Harris⁸, A. David Smith⁹, Gordon Wilcock⁹, Donald Warden⁹ and Clive Holmes¹⁰

¹Schools of Life Sciences and Medicine, University of Nottingham, Nottingham NG7 2UH, UK, ²Institute of Brain, Behaviour and Mental Health, Faculty of Medical and Human Sciences, University of Manchester, Manchester M13 9PT, UK, ³Centre for Public Health, School of Medicine, Queen's University Belfast, BT9 7BL, UK, ⁴Royal Derby Hospital, Derby DE22 3WQ, UK ⁵Department of Psychiatry, University of Bonn, Bonn 53105, Germany, ⁶School of Clinical Sciences, John James Laboratories, University of Bristol, Bristol BS16 1LE, UK, ⁷Salford Royal NHS Foundation Trust, ⁸Cerebral Function Unit, Greater Manchester Neurosciences Centre, Salford Royal Hospital, Stott Lane, Salford M6 8HD, UK, ⁹University of Oxford (OPTIMA), Oxford OX3 9DU, UK ¹⁰Clinical and Experimental Science, University of Southampton, Southampton SO17 1BJ, UK.



Fig. 1

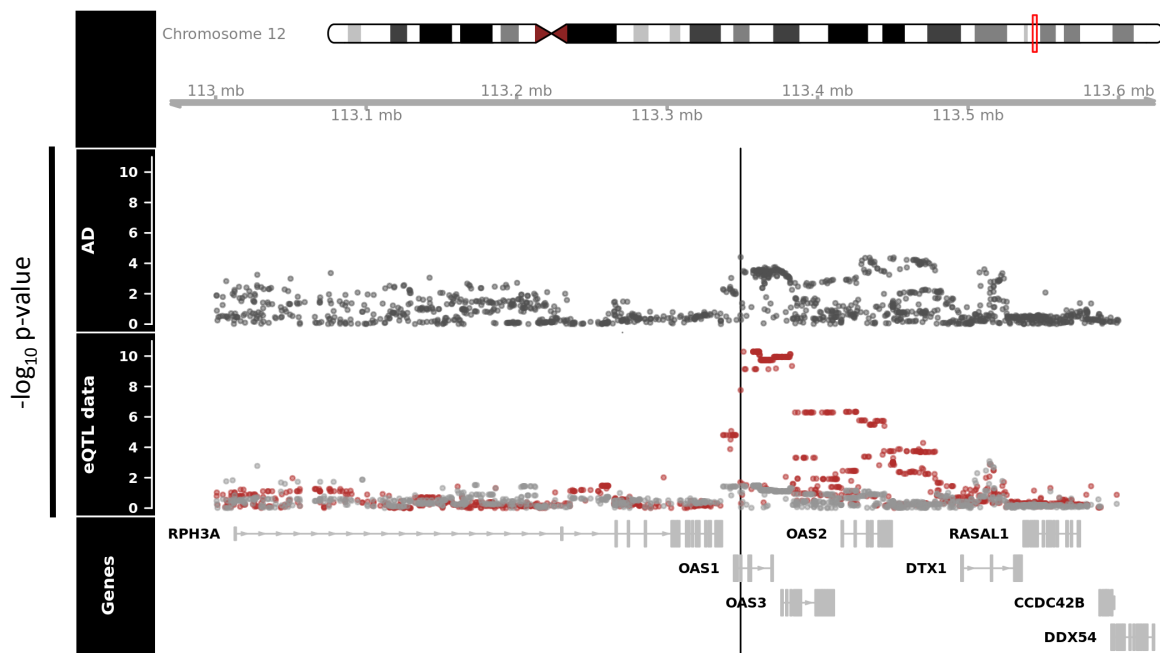


Fig. 2

Mouse symbol (MGI)	Human symbol (HGNC)	NCBI ID	Human Chromosome	Start Location	End Location	Number of SNPs	Gene p-value (adj for GC)	Best SNP	Best SNP Location	Best SNP p-value	Effect size	Risk Allele	Frequency
Predicted genes													
<i>Laptm5</i>	<i>LAPTM5</i>	7805	1	31205315	31230683	45	0.00285	rs1623695	31210852	0.000764	-0.0817	T	0.2065
<i>Cxcl10</i>	<i>CXCL10</i>	3627	4	76942271	76944650	6	0.00227	rs8878	76942300	0.00144	0.0508	A	0.4657
<i>Oas1a</i>	<i>OAS1</i>	4938	12	113344739	113357712	17	0.000388	rs1131454	113348870	3.92E-05	0.1004	A	0.5655
<i>Itgam</i>	<i>ITGAM</i>	3684	16	31271288	31344213	151	0.00571	rs9928397	31320901	0.000671	0.1079	T	0.0894
<i>Lilrb4a</i>	<i>LILRB4</i>	11006	19	55174124	55179848	22	0.00666	rs731170	55176262	0.000272	0.0683	A	0.3054
Established GWAS genes													
<i>H2-Ob</i>	<i>HLA-DOB</i>	3112	6	32780540	32784825	35	0.00354	rs2070121	32781554	0.00138	0.0931	A	0.0796
<i>Trem2</i>	<i>TREM2</i>	54209	6	41126246	41130922	1	0.00258	rs7748513	41127972	0.00182	-0.1293	A	0.9633
<i>Spi1</i>	<i>SPI1</i>	6688	11	47376409	47400127	47	1.34E-06	rs10437655	47391948	1.99E-06	0.0759	A	0.4037
<i>Ms4a6d</i>	<i>MS4A6A</i>	64231	11	59939080	59950674	22	3.07E-10	rs7935829	59942815	1.64E-10	0.1011	A	0.5989
<i>Abi3</i>	<i>ABI3</i>	51225	17	47287589	47300587	37	0.00228	rs2158512	47290253	9.22E-07	0.154	T	0.726
<i>Cd33</i>	<i>CD33</i>	945	19	51728335	51743274	23	1.95E-06	rs12459419	51728477	6.49E-08	-0.0945	T	0.3102

Table 1. The genes predicted to contain SNP variants associated with AD together with established loci associated with AD from GWAS.